17 July 2002

Chemical Physics Letters 360 (2002) 429–435

CHEMICAL PHYSICS LETTERS

www.elsevier.com/locate/cplett

Large scale production of short functionalized carbon nanotubes

Z. Kónya [a,*], I. Vesselenyi [a], K. Niesz [b], A. Kukovecz [a], A. Demortier [b], A. Fonseca [b], J. Delhalle [b], Z. Mekhalif [b], J. B.Nagy [b], A.A. Koós [c], Z. Osváth [c], A. Kocsonya [d], L.P. Biró [c], I. Kiricsi [a]

[a] *Department of Applied and Environmental Chemistry, University of Szeged, Rerrich Bela ter 1., H-6720 Szeged, Hungary*
[b] *Facultés Universitaires Notre-Dame de la Paix, 61 rue de Bruxelles, B-5000 Namur, Belgium*
[c] *Research Institute for Technical Physics and Materials Science, H-1525 Budapest, P.O. Box 49, Hungary*
[d] *KFKI Research Institute for Particle and Nuclear Physics, H-1525 Budapest, P.O. Box 49, Hungary*

Received 18 April 2002

Abstract

A simple mechano-chemical modification of multiwall carbon nanotubes is described. The use of ball-milling in specific atmosphere allows us to introduce functional groups like thiol, amine, amide, carbonyl, chlorine, etc. onto carbon nanotubes. The resulted functional groups are characterized using infrared spectroscopy and X-ray photoelectron spectroscopy. © 2002 Elsevier Science B.V. All rights reserved.

Since their discovery in 1991 [1], carbon nanotubes (NTs) have attracted great attention because of their unique mechanical and electronic properties. Various potential applications involving carbon nanotubes including field emission [2], nanoelectronic devices [3], probe tips for scanning probe microscopy [4], reinforced materials [5,6], hydrogen storage [7], etc. have been proposed. In many of these applications [5,8], it is very important to have either uniform size or reactive functional groups on the outer surface of MWNTs or both requirements. In this communication, we present the formation of thiol, amine and amide, chloride, carbonyl, thiomethoxy, and acyl chloride functional groups on multiwall carbon nanotubes (MWNTs) of semi uniform length, using a mechano-chemical process.

MWNTs were synthesized by catalytic decomposition of acetylene on alumina supported Co/Fe catalyst as described elsewhere [9]. The MWNT sample was purified in two steps. First, the alumina support was dissolved by refluxing in sodium hydroxide solution for two days. In the next step the metal traces were dissolved by stirring the carbon sample in concentrated hydrochloric acid for 5 h. The two steps were repeated twice in order to remove all catalyst traces. Finally, the MWNTs

* Corresponding author. Present address: Lawrence Berkeley National Lab., University of California at Berkeley, 1 Cyclotron road, MS-66, Berkeley, CA 94720, USA; Fax: +1-510-643-9668.

E-mail addresses: konya@chem.u-szeged.hu, zkonya@lbl.gov (Z. Kónya).

0009-2614/02/$ - see front matter
PII: S0009-2614(02)00900-4

were washed with distilled water until a neutral pH was reached.

Using metal mortar, even if its construction material is a special metal alloy, the question arises: is there any metal in the nanotube samples after the reaction? The metal content of the MWNT containing material was checked by X ray fluorescence spectroscopy (XRF) after catalyst and catalyst support removal, after ball-milling in ambient atmosphere for 100 h in a ball mill with stainless steel balls, and after a second step of chemical purification performed to eliminate the amorphous material produced during milling. The measurement was carried out as reported earlier [10]. A Cd-109 radioisotope induced X-ray spectrometer was used and the characteristic X-rays were detected by a Canberra 7333 E detector. It was found that the most significant impurities are Co and Fe. The magnitude of Co and Fe content changes during these treatments as shown in Table 1. Some of the catalyst metals can be trapped inside the hollow channels of the nanotubes and the chemical elimination of this impurity is not possible unless the nanotubes themselves are completely destroyed [11]. The increase of Fe content during the ball-milling by almost an order of magnitude and a moderate increase in the Co content, too is attributed to impurification by the mill material. The impurities introduced during the milling process are removed very efficiently by the second step of chemical purification. It is worth pointing out that the Co content after ball-milling and purification is lower than before the milling, this shows that due to the opening of the tubes, some of the Co encapsulated in the nanotubes could be eliminated after it was made accessible.

In order to obtain more information from the breaking process, two different mills were used. The first mill was an agate mortar with a big agate ball, while the second is a special heatable metal mortar with several small metal balls. In the agate mortar the maximum weight of the sample was about 500 mg, while in the metal 100 g of nanotubes was treated. The MWNT samples before and after functionalization were characterized by X-ray photoelectron spectroscopy (XPS), infrared spectroscopy (IR), volumetric adsorption techniques and transmission electron microscopy (TEM).

Table 1
Iron and cobalt content of a general ball milled sample before and after the milling process

Metal	First purification (wt%)	Ball-milling (wt%)	Second purification (wt%)
Fe	0.09	0.80	0.12
Co	0.15	0.20	0.07

The functionalization of the carbon nanotubes was performed as follows: first, the nanotubes were placed in a ball-mill and the system was degassed by heating either in nitrogen atmosphere or in vacuum. Then, the reactant gas was flown over the nanotube sample for the entire duration of the ball-milling process. Finally, the excess reactant gas was removed either using nitrogen stream or evacuating the system for 1 h. The samples after treatment were washed with ethanol.

Fig. 1 shows TEM images of MWNTs before and after different ball-milling processes. In Fig. 1A, the MWNTs are very long (>10 μm) while Figs. 1a–d show the broken functionalized nanotubes. Comparing the two mill-systems it could be observed that using the metal mill the final average length is about 200–300 nm, while using the agate mortar the nanotubes were 3–4 times longer. It is worth noting that the duration of treatment controls the length of the tubes [12,13], however, after a certain time no more decrease of the average length of the nanotubes was observed. The final length was reached in 18–24 h for the agate mortar and in 5 days for the metal mill. The observed differences in final nanotube length can be explained by the different geometry and construction materials of the two mills. After the breaking process some amorphous carbon was observed, as well. It was found, that the longer the reaction time the more amorphous carbon was formed, for example after two weeks reaction about 30–35% was the amorphous content, but this effect can easily be avoided using the proper reaction time.

During the breaking the apparent density increases by about two order of magnitude. This originates from the disappearance of 'air bubbles'

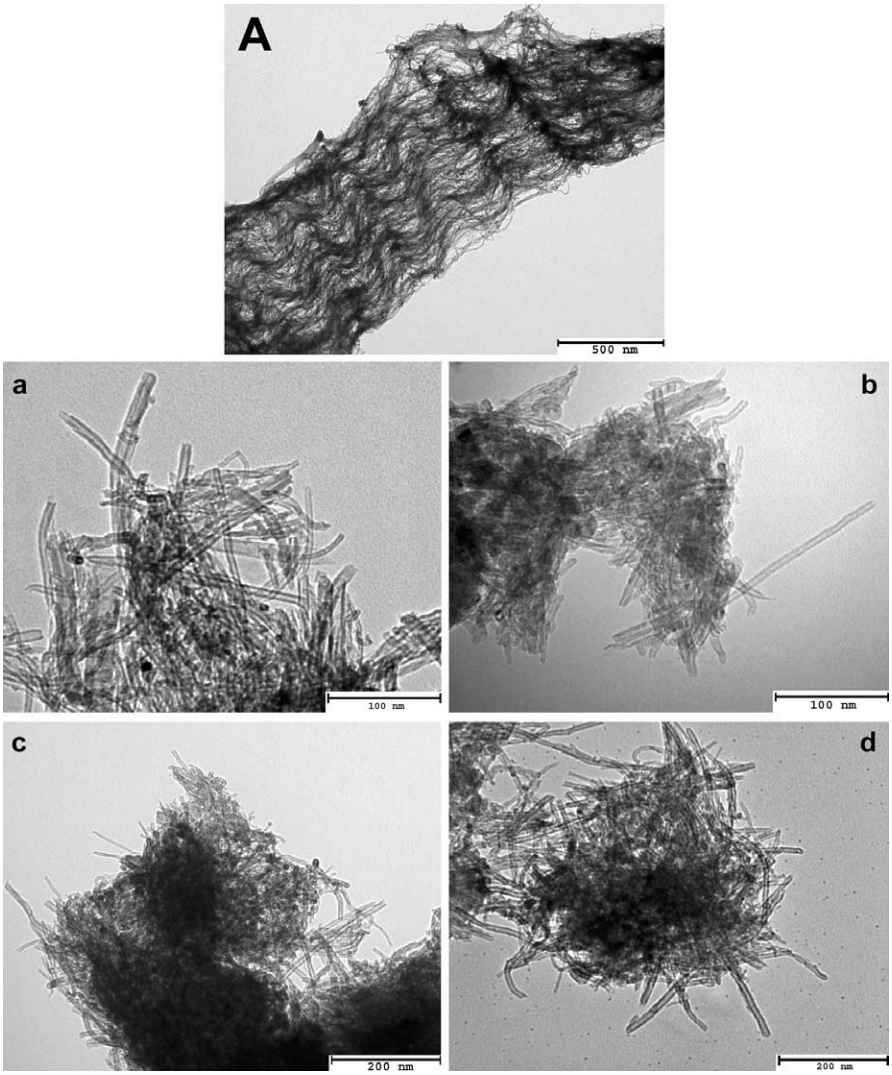

Fig. 1. TEM images of MWNTs before treatment (A) and after ball-milling in Cl_2 (a), NH_3 (b), Cl_2 (c) and CO (d) atmosphere.

present in the web-like nanotube samples before treatment (Fig. 1A $\leftrightarrow$ Fig. 1a). It is noteworthy that this increase in apparent density is very promising in the applications of nanotubes as polymer fillers since the homogenization becomes easier.

The results of the volumetric adsorption measurements confirm that the nanotubes have been physically altered by the milling process. While the specific surface area of pure MWNTs is around 250 m^2/g, after the treatment (breaking and functionalization) this value increases significantly. The calculated pore radius is 20 ± 0.9 Å after breaking, irrespective of the reactant atmosphere. According to the results obtained from the volumetric adsorption measurements it follows that the nanotubes have open ends and the inner pores are accessible after functionalization.

All characterization techniques coincidently showed the formation of uniform size functionalized carbon nanotubes. Table 2 shows the specific surface areas, the pore radii, the functional groups formed during the treatment and the characteristic IR bands of ball-milled NTs.

Table 2
BET surface area, pore radius and functional group generated by reactive ball-milling

Sample	Reactant	BET (m^2/g)	R_p (Å)	Functional groups	IR band (cm^{-1})	Binding energy (eV)
MWNTs	–	254	–	–	–	–
Broken MWNTs	–	290	20	–	–	–
Broken MWNTs	H_2S	288	20	—SH	791	163.6
Broken MWNTs	NH_3	276	20	$—NH_2$, $—CONH_2$	1490	398.8, 400.3
Broken MWNTs	Cl_2	192	20	—Cl	–	199.9
Broken MWNTs	CO	283	20	>C=O	1675	532.5
Broken MWNTs	CH_3SH	294	20	$—SCH_3$	615	163.7
Broken MWNTs	$COCl_2$	278	20	—COCl	1785	198.1

Upon deconvoluting the C_{1s} XPS spectra [14] of NH_3-functionalized MWNTs, five peaks are obtained (Fig. 2). The first one is observed at 284.5 (±0.1) eV and is due to sp^2-hybridized carbon atoms and carbon atoms bonded to hydrogen atoms. The peaks for sp^3-hybridized carbon atoms are centered at 285.1 (±0.1) eV. The peaks at 286.1 (±0.2) eV, 287.4 (±0.2) eV and 289.0 (±0.1) eV represent, the carbon atoms bonded to one oxygen atom by a single bond (e.g., alcohol, ether), by a double bond (e.g., ketone, aldehyde, amide) and to two oxygen atoms (e.g., ester, carboxylic acid), respectively. The peak at 291.0 (±0.1) eV is characteristic of the shake-up of the sp^2-hybridized carbon atoms.

The S_{2p} XPS spectra of MWNTs which have been treated with H_2S shows one component at 163.6 (±0.2) eV. This value corresponds to mercaptans. The deconvolution of N_{1s} XPS spectra of ammonia treated MWNTs shows two species: the first at 399.0 eV and the second at 400.5 eV. The first peak is attributed to amine functional groups and the second is due to the presence of amide [15] (Fig. 2).

In different samples infrared absorption peaks were observed at 791, 1490, 1675, 615 and 1785 cm^{-1}, which can be assign to —SH, $—NH_2$, C=O, $—SCH_3$ and —C(=O)Cl, respectively. The samples for IR spectroscopy were used in KBr as a very diluted solution in order to avoid the problems arising from conductivity. Fig. 3 shows the IR spectra of NH_3-treated sample where the symmetrical and asymmetrical $—NH_2$ vibrations can be observed at 1490 and 894 cm^{-1}, respectively.

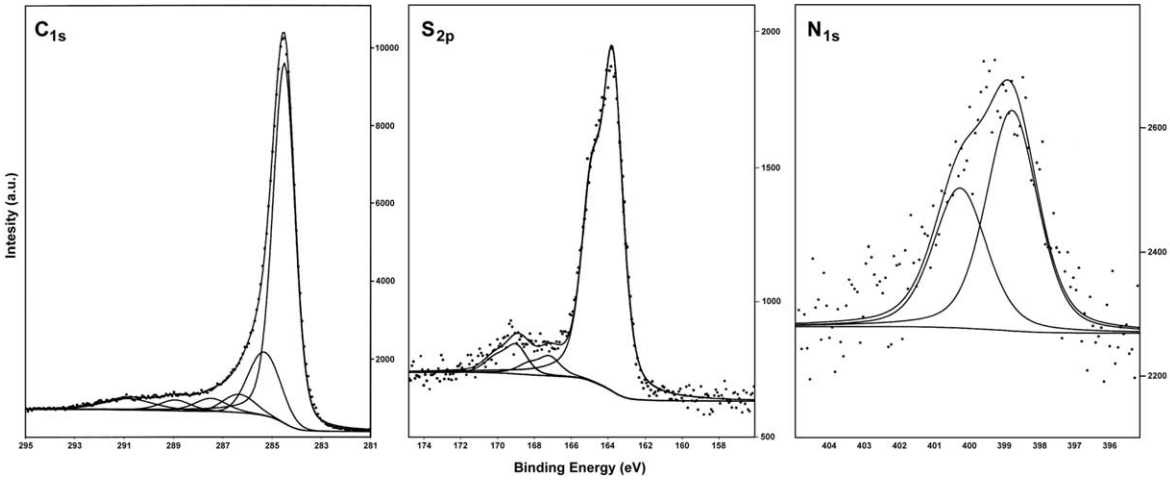

Fig. 2. C_{1s}, S_{2p} and N_{1s} XPS spectra of NH_3, CH_3SH, and NH_3-treated MWNT samples.

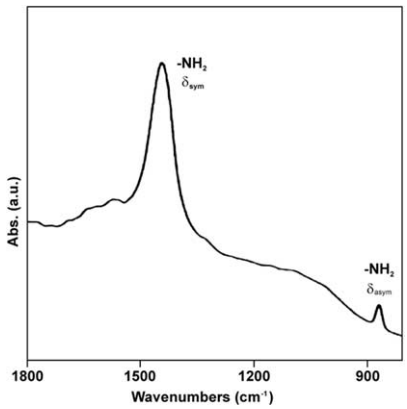

Fig. 3. IR spectra of MWNTs treated in NH_3.

The samples ball milled in NH_3 were investigated as supported samples by Scanning Tunneling Spectroscopy (STM) in topographic and spectroscopic mode (Scanning Tunneling Spectroscopy, STS), too. The nanotubes were ultrasonicated in toluene and droplets of suspension were placed on highly oriented pyrolytic graphite (HOPG) or epitaxial Au evaporated onto mica. The STM images were acquired using commercial Pt/Ir tips with setpoint currents of 200 pA at a bias of 1 V. On the nanotube surface there were observed small 'islands' of functional groups which are bound to defects (Fig. 4). The functional groups attached in a grouped-together way indicate that the anchoring points of the functionalities are the regions with high defect concentrations. The STM measurements cannot decide if these are defects originate from growth, or are created during the ball-milling process. Due to the presence of the functionalized islands, the exterior wall of the carbon nanotube cannot come close enough to the HOPG surface to establish a strong enough Van der Waals interaction, which would fix the nanotube on the support. This manifests itself in the instability of the short tube pieces under the scanning tip. As seen in the two consecutive images, the functionalized nanotube is shifted by the scanning tip over the marker cut in the HOPG.

The typical apparent height of islands of functional groups is of the order of 0.3 nm (Figs. 5a and b). As one may note in the figure, while over the defect-free, not functionalized part of the nanotube the usual atomic resolution STM image is obtained, on the top of the island attached by functionalization no regular structure is observed. The current–voltage spectroscopy (STS) shows that the not functionalized part of the nanotube exhibits a symmetric density of states on the positive and negative side of the Fermi energy situated at zero bias, while the density of states above the Fermi level increases due to functionalization with NH_3 (Fig. 5c).

The experimental results indicate that ball-milling in a controlled ambient leads to function-

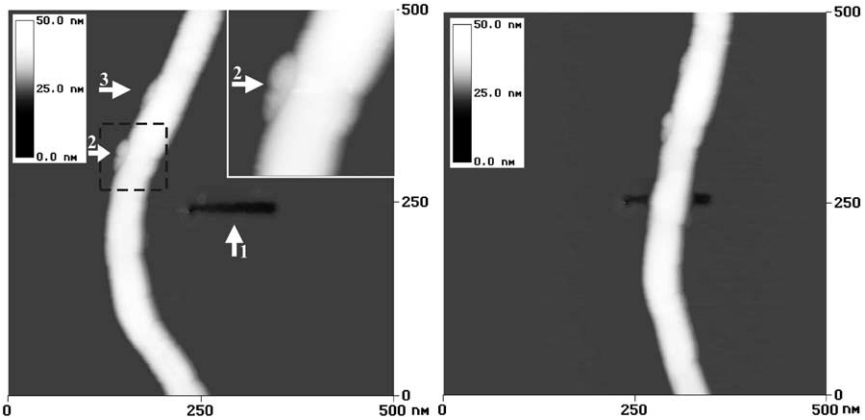

Fig. 4. Two consecutive topographic STM images of a functionalized nanotube shifted by the scanning tip on HOPG. The marker (horizontal line, arrow labeled 1) was cut in the HOPG surface with the STM tip at a bias of 10 V. The horizontal arrows, 2 and 3, point 'islands' of functional groups on the nanotube. The region from the dashed square is shown with a higher magnification in the inset.

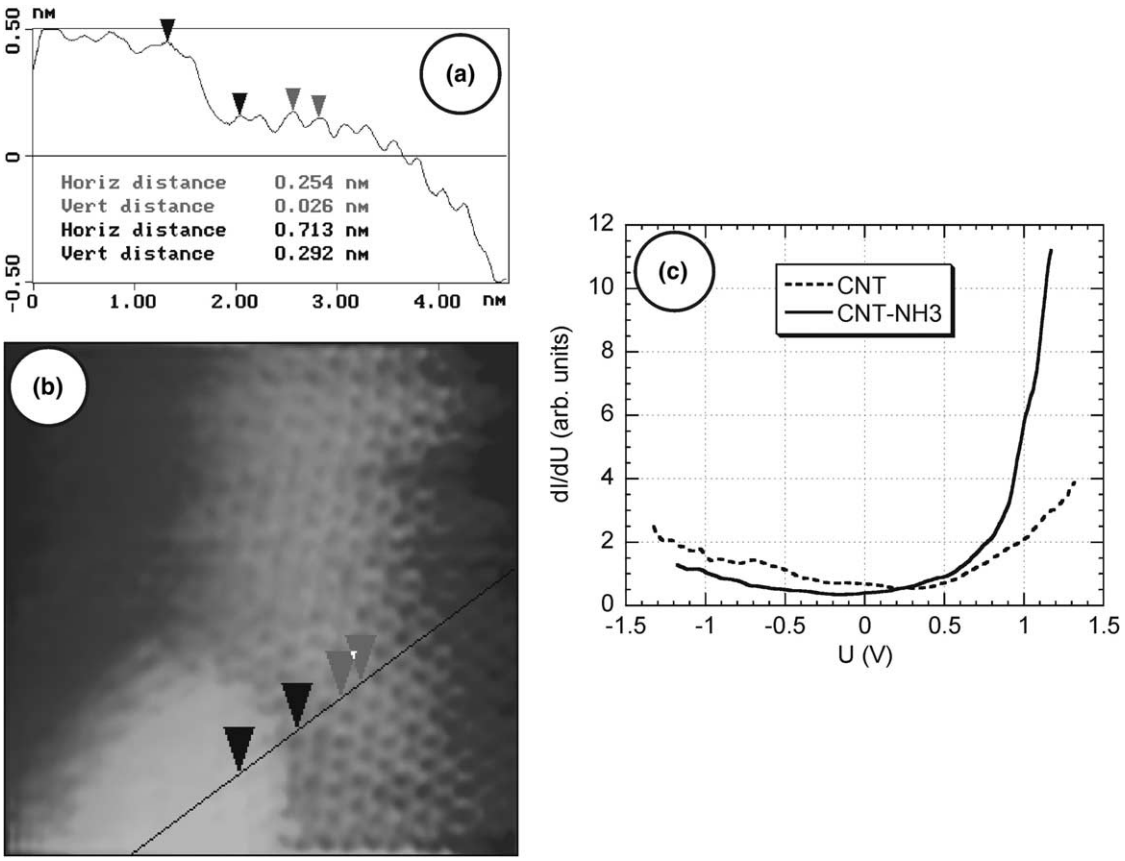

Fig. 5. Topographic STM image and STS data. (a) Line cut on the topographic STM image shown in (b) of a MWNT after ball-milling in NH_3 atmosphere. Setpoint: $I_t = 200$ pA; $U_b = 1$ V. (c) STS over an island of functional groups. STS over a defect-free region is shown for comparison (dashed line).

alization of the carbon nanotubes. If two different ball-milling systems are compared it seems that the efficiency of breaking depends on the geometry of the mill and the duration of the treatment. Cleavage starts not only at defects, but also the mechanical stress induces the formation of defects and, finally, the cleavage of the tubes. It is easy to understand that if the cleavage of the C–C bonds takes place in the presence of NH_3, Cl_2, H_2S, etc., new bonds between the carbon nanotubes and the reactant can easily be formed, albeit the efficiency of the reaction strongly depends on the reactant.

In conclusion, the ball-milling induces functionalization of MWNTs in reactive atmospheres enabled the production of uniform short carbon nanotubes containing different chemical functional groups such as amine, amide, thiol, mercapto, etc. The solid material obtained after various gaseous treatments contained functional groups in rather high quantity. The process can be carried out on large scale – up to 100 grams per reaction. The introduction of different functional groups was confirmed by IR and XPS results. Work is in progress to characterize other functional groups which can be easily introduced by this technique. Moreover, our preliminary results suggest that this technique can be applied not only for multiwall but also for singlewall nanotubes.

Acknowledgements

This work was supported by the EC, contract NANOCOMP, HPRN-CT-2000-00037, and by

EC Centre of Excellence program (no. ICA1-CT-2000-70029), by the Belgian Programme PAI P4/10. A.D. thanks F.R.I.A. for financial help. Z.K. and I.K. acknowledge support from FKFP 0216/2001, F 038249, T 037952 and Bolyai fellowship, L.P.B. acknowledges support from OTKA grant T 30435 in Hungary.

References

[1] S. Iijima, Nature 354 (1991) 56.
[2] J.-M. Bonard, H. Kind, T. Stöckli, L.-O. Nilsson, Solid State Electron. 45 (2001) 893.
[3] S. Roth, M. Burghard, V. Krstic, K. Liu, J. Muster, G. Philipp, G.T. Kim, J.G. Park, Y.W. Park, Curr. Appl. Phys. 1 (2001) 56.
[4] S. Wong, A. Woolley, E. Joselevich, C. Lieber, Chem. Phys. Lett. 306 (1999) 219.
[5] P. Ajayan, L. Schalder, C. Giannaris, A. Rubio, Adv. Mater. 12 (2000) 750.
[6] Z. Jin, K.P. Pramoda, G. Xu, S.H. Goh, Chem. Phys. Lett. 337 (2001) 43.
[7] M. Hirscher, M. Becher, M. Haluska, A. Quintel, V. Skakalova, Y.-M. Choi, U. Dettlaff-Weglikowska, S. Roth, I. Stepanek, P. Bernier, A. Leonhardt, J. Fink, J. Alloys Compd. 330–332 (2002) 654.
[8] Z. Liu, Z. Shen, T. Zhu, S. Hou, L. Ying, Z. Shi, Z. Gu, Langmuir 16 (2000) 3569.
[9] I. Willems, Z. Konya, J.-F. Colomer, G. Van Tendeloo, N. Nagaraju, A. Fonseca, J. B.Nagy, Chem. Phys. Lett. 317 (2000) 71.
[10] L.P. Biró, N.Q. Khanh, Z. Vértesy, Z.E. Horváth, Z. Osváth, A. Koós, J. Gyulai, A. Kocsonya, Z. Kónya, X.B. Zhang, G. Van Tendeloo, A. Fonseca, J. B.Nagy, Mat. Sci. Eng. C 19 (2002) 9.
[11] L.P. Biró, N.Q. Khanh, Z.E. Horváth, Z. Vértesy, A. Kocsonya, Z. Kónya, Z. Osváth, A. Koós, J. Gyulai, X.B. Zhang, G. Van Tendeloo, A. Fonseca, J. B.Nagy, in: H. Kuzmany, J. Fink, M. Mehring, S. Roth (Eds.), XVth International Winterschool on Electronic Properties of Novel Materials an Euroconference: Molecular Nanostructures, American Institute of Physics Proceedings Series, vol. 591, 2001, p. 183.
[12] N. Pierard, A. Fonseca, Z. Konya, I. Willems, G. Van Tendeloo, J. B.Nagy, Chem. Phys. Lett. 335 (2001) 1.
[13] G. Maurin, I. Stepanek, P. Bernier, J.-F. Colomer, J. B.Nagy, F. Henn, Carbon 39 (2001) 1273.
[14] H. Ago, T. Kugler, F. Cacialli, W. Salaneck, M. Shaffer, A. Windle, R. Friend, J. Phys. Chem. B 103 (1999) 8116.
[15] G. Xu, Y. Hibino, M. Aoki, K. Awazu, M. Tanihara, Y. Imanishi, Colloids Surf. B 19 (2000) 249.